End-depth in inverted semicircular channels: experimental and theoretical studies

Subhasish Dey[1], D. Nagesh Kumar[2] and D. Ram Singh[1]

[1]Department of Civil Engineering, Indian Institute of Technology, Kharagpur 721302, West Bengal, India
E-mail: *sdey@civil.iitkgp.ernet.in*
[2]Department of Civil Engineering, Indian Institute of Science, Bangalore 560012, India

Abstract The flow upstream of a free overfall from smooth inverted semicircular channels is theoretically analysed to compute the end-depth ratio (EDR), applying an energy equation based on the Boussinesq assumption. This approach eliminates the need for an experimentally determined pressure coefficient. Experiments were conducted with horizontal channel conditions. The EDR related to the critical depth, which occurs upstream from the end section, is found to be around 0.695 for a critical depth-diameter ratio up to 0.40. A simple method is presented to estimate the discharge from a known end-depth. The theoretical model corresponds closely with the experimental data.

Keywords End-depth; flow measurement; free overfall; free surface flow; open channel flow; steady flow

Introduction

A free overfall offers the possibility of being used as a flow-measuring device in an open channel. As, in hydrologic engineering, it is essential to measure discharge in open channels, considerable attention has been paid to exploring free overfall in different shaped channels. In free overfalls, the water nappe emerging out is affected by the gravity resulting in an accelerated flow. With the atmospheric pressure existing above and below the nappe, the water surface profile is a parabola. At the end section, this causes a pressure distribution to depart from the hydrostatic pressure distribution. At sections upstream from the brink, the water surface curvature gradually decreases (Wilkinson 1973) and at an upstream control section the hydrostatic pressure is reestablished. As a result of which, the flow depth reduces gradually from the upstream control section towards the downstream direction with a minimum depth h_e occurring at the brink, termed the *end-depth*. In subcritical flow, a critical section occurs if the flow has to pass through a supercritical state. The critical depth h_c based on hydrostatic pressure distribution occurs upstream from the brink.

Fundamental experimental research was carried out by Rouse (1936) to determine the end-depth ratio (EDR=end-depth/critical depth), which was found to be 0.715 in mildly sloping rectangular channels. Since then numerous experiments on free overfalls in different channels have been reported (Diskin 1961, Smith, 1962, Rajaratnam and Muralidhar 1964a, b, Clarke 1965, Anderson 1967, Hager 1983, Keller and Fong 1989, Anastasiadou-Partheniou and Hatzigiannakis 1995, Dey 1998a, b, 2000, 2001a, b, Dey and Ravi Kumar 2002). However, no attempt has so far been made to analyse free overfall in inverted semicircular channels. Though the section is not common, inverted semicircular tunnels or sewers are found in some places in India, especially in the southern part. Among them the Pasuvemula tunnel at four miles along the Nagarjuna Sagar right canal (in the Guntur district in Andhra Parades, India) and the Ramasagaram tunnel on the Tungabhadra low level canal (in the Bellery district in Karnataka, India) are pertinent. Some other semicircular tunnels are also in the Nagarjuna Sagar and Krishna Sagar dams.

This paper presents a theoretical model for a free overfall from smooth inverted semicircular channels, applying an energy equation based on the Boussinesq assumption (see the appendix). It eliminates the need for an empirical pressure coefficient. The model yields the EDR and the discharge, which are verified by the experimental results in subcritical flow. This study does not consider the supercritical flow case, as it is not common in practice.

Experimental set-up and procedure

The experiments were carried out in three different inverted semicircular channels (made of transparent Perspex), having diameters of 128 mm (channel 1), 68 mm (channel 2) and 43 mm (channel 3). The lengths of the channels were 3 m. Perspex walls enabled observations to be made of the flow. A suitable holding arrangement was made to hold the channel. As, in this study, the end-depths for the subcritical approaching flow were explored, the experimental runs were taken in the horizontal channel condition. The channel was connected to an upstream supply through a stilling tank to eliminate water surface fluctuations. Water entered the stilling tank from a constant head tank fed by a centrifugal pump. Water discharged through the downstream end of the channel into a measuring tank and finally drained out into the reservoir. A valve in the upstream supply line controlled the discharge. The discharge was set by slowly opening the upstream valve until a desirable height at the end of the channel resulted. Once this was reached, the corresponding discharge was recorded with the aid of a measuring tank, where the water was collected for a predetermined period of time. A diverter helped to divert the water from the measuring tank to a drain connected to the reservoir or vice versa. The end-depths were measured carefully by a Vernier point gauge just touching the water surface with an accuracy of ± 0.1 mm. Similar point gauges were used to record the difference in water surface level in the measuring tank. However, time and care taken during the measurements ensured the accuracy. Tables 1(a)–(c) present the experimental data collected in channels under the horizontal condition.

Table 1(a) Experimental data collected in Channel 1

Channel	D (mm)	Q (m³s⁻¹)	$\hat{h}_c$	$\hat{h}_e$	$\tilde{h}_e$	$\hat{Q}$
		4.604×10^{-4}	0.086	0.059	0.691	2.508×10^{-2}
		5.279×10^{-4}	0.094	0.066	0.706	2.875×10^{-2}
		6.442×10^{-4}	0.107	0.078	0.726	3.509×10^{-2}
		6.900×10^{-4}	0.112	0.082	0.728	3.758×10^{-2}
		2.083×10^{-3}	0.234	0.169	0.721	1.135×10^{-1}
		1.875×10^{-3}	0.218	0.149	0.684	1.021×10^{-1}
		1.701×10^{-3}	0.205	0.148	0.721	9.305×10^{-2}
		1.438×10^{-3}	0.183	0.124	0.677	7.830×10^{-2}
		8.429×10^{-4}	0.128	0.090	0.703	4.591×10^{-2}
		1.233×10^{-3}	0.165	0.118	0.717	6.718×10^{-2}
1	128	1.029×10^{-3}	0.146	0.100	0.684	5.606×10^{-2}
		8.933×10^{-4}	0.133	0.098	0.734	4.866×10^{-2}
		7.771×10^{-4}	0.121	0.068	0.679	4.233×10^{-2}
		4.171×10^{-4}	0.080	0.055	0.680	2.272×10^{-2}
		2.179×10^{-3}	0.241	0.176	0.739	1.187×10^{-1}
		1.954×10^{-3}	0.224	0.161	0.719	1.064×10^{-1}
		5.829×10^{-4}	0.100	0.071	0.707	3.175×10^{-2}
		1.763×10^{-3}	0.209	0.143	0.681	9.600×10^{-2}
		1.550×10^{-3}	0.192	0.136	0.706	8.443×10^{-2}
		1.183×10^{-3}	0.161	0.109	0.680	6.445×10^{-2}

74

Table 1(b) Experimental data collected in Channel 2

Channel	D (mm)	Q (m^3s^{-1})	$\hat{h}_c$	$\hat{h}_e$	$\tilde{h}_e$	$\hat{Q}$
		7.558×10^{-4}	0.337	0.231	0.685	1.998×10^{-1}
		5.158×10^{-4}	0.264	0.191	0.722	1.366×10^{-1}
		4.233×10^{-4}	0.232	0.163	0.704	1.121×10^{-1}
		2.804×10^{-4}	0.177	0.124	0.701	7.425×10^{-2}
		3.821×10^{-4}	0.217	0.158	0.727	1.012×10^{-1}
		2.521×10^{-4}	0.164	0.121	0.735	6.675×10^{-2}
		2.258×10^{-4}	0.153	0.104	0.678	5.980×10^{-2}
		5.988×10^{-4}	0.291	0.200	0.688	1.585×10^{-1}
		4.604×10^{-4}	0.245	0.178	0.728	1.219×10^{-1}
2	68	4.250×10^{-4}	0.232	0.165	0.708	1.125×10^{-1}
		7.454×10^{-4}	0.334	0.236	0.706	1.974×10^{-1}
		6.475×10^{-4}	0.306	0.223	0.729	1.714×10^{-1}
		5.550×10^{-4}	0.277	0.187	0.674	1.470×10^{-1}
		4.954×10^{-4}	0.257	0.181	0.740	1.312×10^{-1}
		4.317×10^{-4}	0.235	0.166	0.706	1.143×10^{-1}
		7.875×10^{-4}	0.345	0.253	0.731	2.085×10^{-1}
		6.842×10^{-4}	0.317	0.223	0.704	1.812×10^{-1}
		6.713×10^{-4}	0.313	0.214	0.683	1.777×10^{-1}
		6.171×10^{-4}	0.296	0.214	0.720	1.634×10^{-1}
		5.800×10^{-4}	0.285	0.195	0.683	1.536×10^{-1}

Table 1(c) Experimental data collected in Channel 3

Channel	D (mm)	Q (m^3s^{-1})	$\hat{h}_c$	$\hat{h}_e$	$\tilde{h}_e$	$\hat{Q}$
		2.495×10^{-4}	0.345	0.247	0.716	2.077×10^{-1}
		2.180×10^{-4}	0.317	0.224	0.708	1.815×10^{-1}
		1.811×10^{-4}	0.282	0.201	0.714	1.508×10^{-1}
		1.586×10^{-4}	0.258	0.180	0.696	1.320×10^{-1}
		1.358×10^{-4}	0.233	0.164	0.705	1.130×10^{-1}
		1.002×10^{-4}	0.191	0.137	0.716	8.344×10^{-2}
		7.095×10^{-5}	0.152	0.104	0.685	5.908×10^{-2}
		6.600×10^{-5}	0.145	0.102	0.703	5.496×10^{-2}
		5.520×10^{-5}	0.128	0.092	0.721	4.597×10^{-2}
3	43	3.660×10^{-5}	0.098	0.067	0.689	3.047×10^{-2}
		2.646×10^{-4}	0.357	0.249	0.697	2.203×10^{-1}
		2.432×10^{-4}	0.339	0.237	0.697	2.025×10^{-1}
		2.829×10^{-4}	0.371	0.261	0.702	2.356×10^{-1}
		2.460×10^{-4}	0.342	0.243	0.710	2.048×10^{-1}
		1.977×10^{-4}	0.297	0.210	0.704	1.646×10^{-1}
		1.682×10^{-4}	0.268	0.186	0.694	1.400×10^{-1}
		1.511×10^{-4}	0.250	0.179	0.714	1.258×10^{-1}
		1.187×10^{-4}	0.213	0.150	0.703	9.880×10^{-2}
		7.815×10^{-5}	0.162	0.115	0.713	6.507×10^{-2}
		4.935×10^{-5}	0.119	0.081	0.681	4.109×10^{-2}

S. Dey et al.

Model for end-depth ratio (EDR)

In a free overfall, the water surface is a continuously falling curve, which starts somewhere upstream of the brink, passes through the brink and ends up with a trajectory of a gravity fall (Figure 1). Based on the Boussinesq assumption for a small free surface curvature, a generalised equation (see the appendix) for the end-depth is given by Subramanya (1987) as

$$6\hat{E}_e - 4\tilde{h}_e - 3f(\tilde{h}_e) = 0 \tag{1}$$

where $\hat{E}_e = E_e/h_c$, E = specific energy, h = flow depth, $\tilde{h}_e = \text{EDR}(= h_e/h_c)$, $f(\tilde{h}_e) = A_c^3/(A_e^2 T_c h_c)$, A = flow area and T = top width of the flow. In the above, subscripts 'e' and 'c' refer to the end and critical sections, respectively.

In subcritical flow, the critical depth is greater than the end-depth but is less than the normal depth. Hence, the critical depth occurs at some distance upstream from the brink. However, there is a continuity of the free surface. For an inverted semicircular channel (Figure 1), the flow area A and the top width T of the flow are given as

$$A = 0.25D^2 \xi(\hat{h}) \tag{2}$$

$$T = D^2 \sqrt{1 - 4\hat{h}^2} \tag{3}$$

where D = diameter of the channel, $\hat{h} = h/D$ and

$$\xi(\hat{h}) = \arcsin(2\hat{h}) + 2\hat{h}\sqrt{1 - 4\hat{h}^2}. \tag{4}$$

In subcritical flow, the critical depth occurs before the end-depth and, as such, h_c exists at some location upstream from the brink. The specific energy at any section is given by

$$E = E_e = E_c = h_c + Q^2/(2gA_c^2). \tag{5}$$

where g = gravitational constant.

Normalising the above equation, one can write

$$\hat{E}_e = 1 + 0.125 \frac{\xi(\hat{h}_c)}{\hat{h}_c \sqrt{1 - 4\hat{h}_c^2}}. \tag{6}$$

Also, $f(\tilde{h}_e)$ can be expressed using Eqs. (2)–(4) as

$$f(\tilde{h}_e) = \frac{A_c^3}{A_e^2 T_c h_c} = 0.25 \frac{\xi^3(\hat{h}_c)}{\xi^2(\hat{h}_e)\hat{h}_c \sqrt{1 - 4\hat{h}_c^2}}. \tag{7}$$

Using Eqs. (6) and (7), Eq. (1) can be solved numerically to estimate EDR $\tilde{h}_e$.
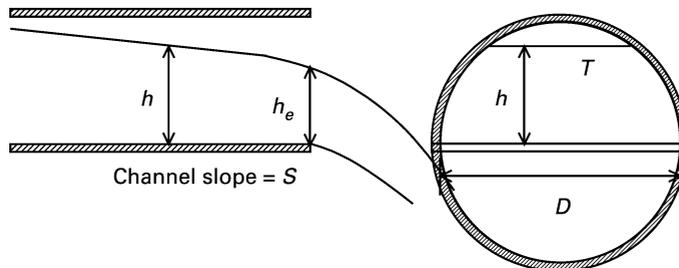

Figure 1 Definition sketch

Model for discharge

Discharge is calculated using the expression of the Froude number, that is

$$F = V/\sqrt{g(A/T)} \tag{8}$$

where V = flow velocity.

As the flow is critical at a location upstream from the brink, using $F = 1$ in Eq. (8) one can express the discharge Q in normalized form as

$$\hat{Q} = \frac{1}{8} \cdot \frac{\xi^{1.5}(\hat{h}_c)}{(1 - 4\hat{h}_c^2)^{0.25}} \tag{9}$$

where $\hat{Q} = Q/(g^{0.5}D^{2.5})$. Eq. (9) is used to calculate $\hat{Q}$ theoretically in subcritical flow, using the known end-depth.

Results

Using Eqs. (6) and (7), Eq. (1) can be solved numerically to compute EDR $\tilde{h}_e$, and subsequently $\hat{Q}$ is determined from Eq. (9). The dependence of $\tilde{h}_e$ on $\hat{h}_c$ obtained from the present model is shown in Figure 2. The curve obtained from the present model lies almost in the middle portion of the experimental data. The value of EDR $\tilde{h}_e$ is around 0.695 up to $\hat{h}_c = 0.40$. The computed curve rises sharply from $\hat{h}_c = 0.40$ and $\tilde{h}_e$ approaches 1 as $\hat{h}_c$ approaches 1. The variation of $\hat{h}_e$ with $\hat{Q}$ is presented in Figure 3. The present model corresponds closely with the experimental observations.

Conclusions

The flow upstream of a free overfall from smooth inverted semicircular channels has been theoretically analysed to calculate the end-depth ratio (EDR), applying an energy equation based on the Boussinesq assumption. This approach has eliminated the need for an empirical pressure coefficient. Experiments were conducted with the horizontal channel condition. The EDR has been related to the critical depth, which occurs upstream from the end section, and the value of the EDR is found to be about 0.695 for a critical depth-diameter ratio up to 0.40. A simple method has been presented to estimate the discharge from a known end-depth. The theoretical model has corresponded closely with the experimental data.
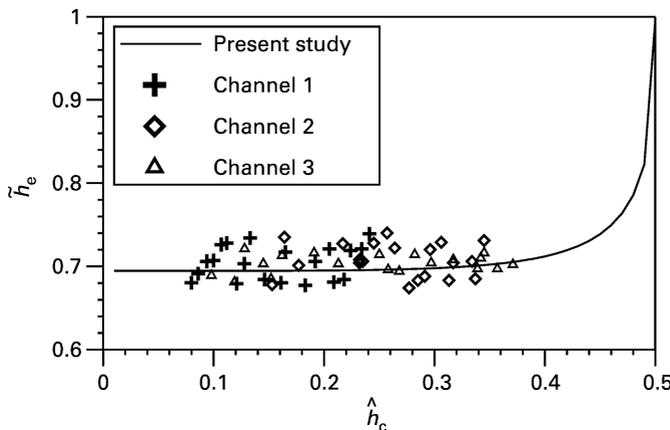

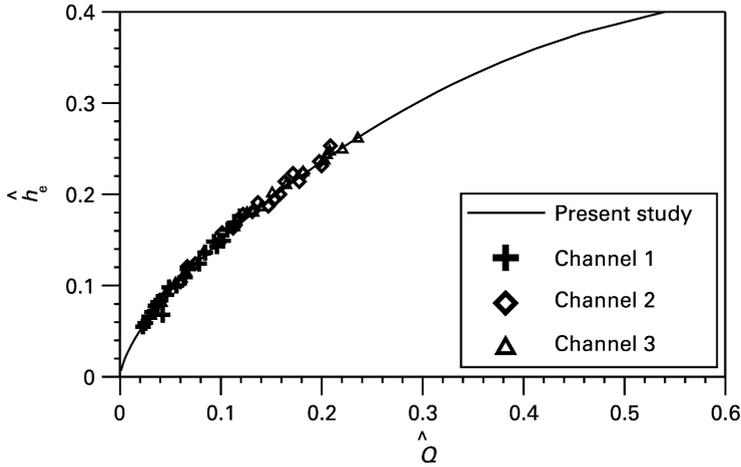**Figure 2** EDR $\tilde{h}_e$ as a function of $\hat{h}_c$ in subcritical flow

77

Figure 3 Variation of $\hat{h}_e$ with $\hat{Q}$ in subcritical flow

Appendix

Boussinesq assumption

The free surface curvature of a free overfall being relatively small it varies from a finite value (convex upwards) at the surface to zero at the channel boundary. According to the Boussinesq assumption (Jaeger, 1957), a linear variation of the streamline curvature with depth is assumed. He expressed the effective hydrostatic pressure head h_{ep} as

$$h_{ep} = h + \frac{kh^2}{3g} \tag{A1}$$

where $k = (V^2/h)(d^2h/dx^2)$ and x = streamwise distance.

Generalised equation of EDR (Subramanya 1987)

The specific energy E_e at the end section is given by

$$E_e = h_{ep} + \frac{V_e^2}{2g} = h_e + \frac{V_e^2 h_e}{3g}\left(\frac{d^2h}{dx^2}\right)_{h=h_e} + \frac{V_e^2}{2g} = h_e + \frac{Q^2 h_e}{3gA_e^2}\left(\frac{d^2h}{dx^2}\right)_{h=h_e} + \frac{Q^2}{2gA_e^2}. \tag{A2}$$

Normalizing Eq. (A2) by h_c and using $Q^2/g = A_c^3/T_c$ yields

$$\left.\frac{d^2(h/h_c)}{d(x/h_c)^2}\right|_{h=h_e} = \frac{3}{\tilde{h}_e f(\tilde{h}_e)}\left[\hat{E}_e - \tilde{h}_e - \frac{1}{2}f(\tilde{h}_e)\right]. \tag{A3}$$

Since the change of free surface curvature is

$$(d^2h/dx^2)_{h=h_e} = -g/V_e^2 \tag{A4}$$

normalizing Eq. (A4) by h_c and using $Q^2/g = A_c^3/T_c$ yields

$$\left.\frac{d^2(h/h_c)}{d(x/h_c)^2}\right|_{h=h_e} = -\frac{1}{f(\tilde{h}_e)}. \tag{A5}$$

Equating Eqs. (A3) and (A5), the following equation is obtained

$$6\hat{E}_e - 4\tilde{h}_e - 3f(\tilde{h}_e) = 0. \tag{A6}$$

The above equation proposed by Subramanya (1987) is the generalised equation of the end-depth ratio (EDR).

References

Anastasiadou-Partheniou, L. and Hatzigiannakis, E. (1995). General end-depth-discharge relationship at free overfall in trapezoidal channel. *J. Irrig. Drain. Engng.*, **121**(2), 143–151.

Anderson, M.V. (1967). Non-uniform flow in front of a free overfall. *Acta Polytechnic Scand.*, **42**, 73–83.

Clarke, N.S. (1965). On two-dimensional inviscid flow in a waterfall. *J. Fluid Mech.*, **22**, 359–369.

Dey, S. (1998a). Free overfall in rough rectangular channels: a computational approach. *Water, Maritime and Energy, Proc. Inst. Civil Engrs (London)*, **130**, 51–54.

Dey, S. (1998b). End depth in circular channels. *J. Hydraul. Engng., ASCE*, **124**(8), 856–863.

Dey, S. (2000). End depth in steeply sloping rough rectangular channels. *Sadhana, Proc. Indian Acad. Sci.*, **25**, 1–10.

Dey, S. (2001a). EDR in circular channels. *J. Irrig. Drain. Engng.*, **127**(2), 110–112.

Dey, S. (2001b). Flow metering by end-depth method in elliptic channels. *Dam Engng.*, **12**(1), 5–19.

Dey, S. and Ravi Kumar, B. (2002). Hydraulics of free overfall in (Δ-shaped channels. Sadhana. *Proc. Indian Acad. Sci.*, **27**, 353–363.

Diskin, M.H. (1961). The end depth at a drop in trapezoidal channels. *J. Hydraul. Div., ASCE*, **87**(4), 11–32.

Hager, W.H. (1983). Hydraulics of the plane overfall. *J. Hydraul. Engng., ASCE*, **109**(2), 1683–1697.

Jaeger, C. (1957). *Engineering Fluid Mechanics*, St. Martin's Press, New York.

Keller, R.J. and Fong, S.S. (1989). Flow measurements with trapezoidal free overfall. *J. Irrig. Drain. Engng., ASCE*, **115**(1), 125–136.

Rajaratnam, N. and Muralidhar, D. (1964a). End depth for exponential channels. *J. Irrig. Drain. Div., ASCE*, **90**(1), 17–36.

Rajaratnam, N. and Muralidhar, D. (1964b). End depth for circular channels. *J. Hydraul. Div., ASCE*, **90**(2), 99–119.

Rouse, H. (1936). Discharge characteristics of the free overfall. *Civil Engng., ASCE*, **6**(4), 257–260.

Smith, C.D. (1962). Brink depth for a circular channel. *J. Hydraul. Div., ASCE*, **88**(6), 125–134.

Subramanya, K. (1987). *Flow in Open Channels*, Tata McGraw Hill, New Delhi.

Wilkinson, D.L (1973). Surface slopes at control sections in open channel flow. *Prog. Rep.* No. 29, ISVA DTH.